Polish J. Chem., **77**, 1461–1471 (2003)

Synthesis, X-ray Crystallography and Computer-Aided Design Study of 5-Amino-3-methylisoxazole-4-carboxylic Acid N-(2,4,6-Trimethylpyridinium)amide Chlorate(VII) Salt and Its Analogues*

by A. Jezierska[1], J. Zygmunt[2], T. Głowiak[1], A. Koll[1] and S. Ryng[2]**

[1]*University of Wrocław, Faculty of Chemistry, 14 F. Joliot-Curie, 50-383 Wrocław, Poland*
[2]*Wroclaw Medical University, Faculty of Pharmacy, Department of Organic Chemistry, 9 Grodzka, 50-137 Wrocław, Poland*

(Received March 20th, 2003; revised manuscript May 8th, 2003)

Experimental and theoretical investigations were performed for 5-amino-3-methylisoxazole-4-carboxylic acid N-(2,4,6-trimethylpyridinium)amide chlorate(VII) salt, which belongs to the group of isoxazole derivatives, potential antibacterial or antifungal agents. The results related to its synthesis and X-ray diffraction are presented. Quantum-chemical DFT calculations were carried out for the title molecule and its analogues. Atomic charges were calculated according to Bader's Atoms In Molecules Theory in order to find the quantum similarities of the molecules. The Polarizable Continuum Model (SCRF/PCM) with water ($\varepsilon = 78.39$) as a solvent was used to determine the environment effects on molecular properties. The solid-state geometry optimization with Geodecker's pseudopotentials and plane-wave basis set was used to compare experimental and calculated geometrical parameters for the title compound.

Key words: isoxazole derivatives, synthesis, SCRF/PCM model, AIM, electrostatic potential, solid-state calculations

The isoxazole derivatives have recently been intensively investigated [1–6]. They are interesting objects from the synthetic, as well as physicochemical, biological and theoretical points of view. The aim of these studies was mainly searching for new compounds with immunological activity. New isoxazole derivatives with such properties have been proposed. The compounds containing the isoxazole moiety exhibit various biological activity, for instance antvirial [7], antibacterial [8] or anticonvulsant [9] as reported in the literature. In this work the synthesis, X-ray crystallography and a theoretical study of 5-amino-3-methylisoxazole-4-carboxylic acid N-(2,4,6-trimethylpyridinium)amide chlorate(VII) salt were performed. In addition to the title compound, its analogues were also analysed in order to establish relations between the structures and physicochemical properties [10] (see Figure 1). The Density Functional Theory (DFT), [11,12], was used as a tool to describe the structures of

---

* Dedicated to Prof. M. Szafran on the occasion of his 70th birthday.

**Author for correspondence: e-mail: saryng@bf.uni.wroc.pl, tel. +48 71 784 03 48, fax: +48 71 784 03 41

the investigated compounds. Compounds **1** and **2** were synthesized, while compounds **3** and **4** were used as models in the theoretical study (*cf.* Figure 1). Compound **1** does not show defined biological activity, while compound **2** exhibits experimentally confirmed immunological properties, *i.e.* it is a stimulator of PHA-induced cell proliferation [4]. The Polarizable Continuum Model (SCRF/PCM) was applied in order to map solvent influence on the molecules [13,14]. The electron densities and electrostatic potentials around the molecules reflect the physical forces determining ligand-acceptor interactions. Atomic charges were calculated for all compounds according to the Atoms In Molecules theory [15]. Additionally, the Wiberg bond index was taken into account [16]. The solid-state geometry optimization was performed using Goedecker's pseudopotentials and the CPMD program [17,18] in order to compare the experimental crystallographic structure with the calculated for 5-amino-3-methylisoxazole-4-carboxylic acid N-(2,4,6-trimethylpyridinium)amide chlorate(VII) salt. The paper consists of two parts. The first contains experimental data: the synthesis and X-ray crystallography results, while the second the molecular modeling study.

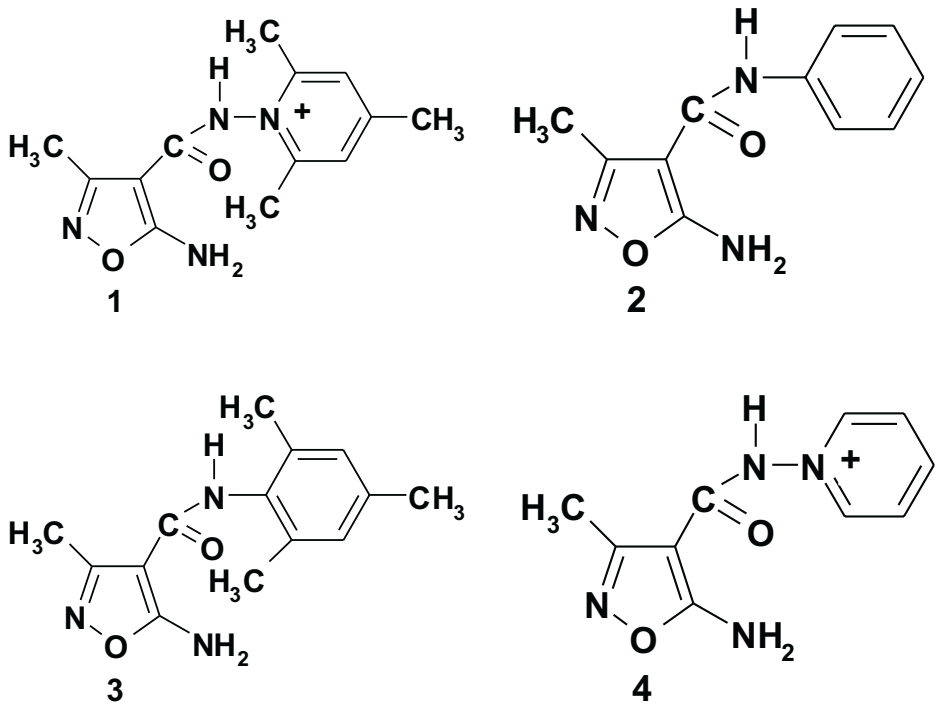

Figure 1. The structures of the theoretically investigated compounds: **1** and **2** were obtained experimentally, while **3** and **4** are models.

EXPERIMENTAL

The synthesis of 5-amino-3-methylisoxazole-4-carboxylic acid N-(2,4,6-trimethylpyridinium)amide chlorate(VII) salt. Commercially available reagents and solvents were used without further purification in order to synthesize the title compound. The initial reactant 5-amino-3-methyl-4-isoxazolecarboxylic acid hydrazide was prepared according to the previously reported method [6,19]. The scheme of synthesis is presented in Figure 2. Three mmol 5-amino-3-methyl-4-isoxazolecarboxylic acid hydrazide, 50 ml isopropanol and 3.3 mmol 2,4,6-trimethylpyrylium chlorate(VII) were placed in a 100 ml round-bottomed flask fitted with a condenser. The reaction mixture was slowly refluxed by stirring for 2 hours, using a hot plate. During the course of the reaction, the mixture becomes clear. When the reaction was complete (controlled by a TLC), the solution was evaporated under diminished pressure to 30 ml. The product was poured into hot THF and filtered off after cooling. The compound was purified by recrystallization in ethanol. Colourless plates of crystalline product were obtained as a result. Compound **2** presented in Figure 1 was synthesized according [4].

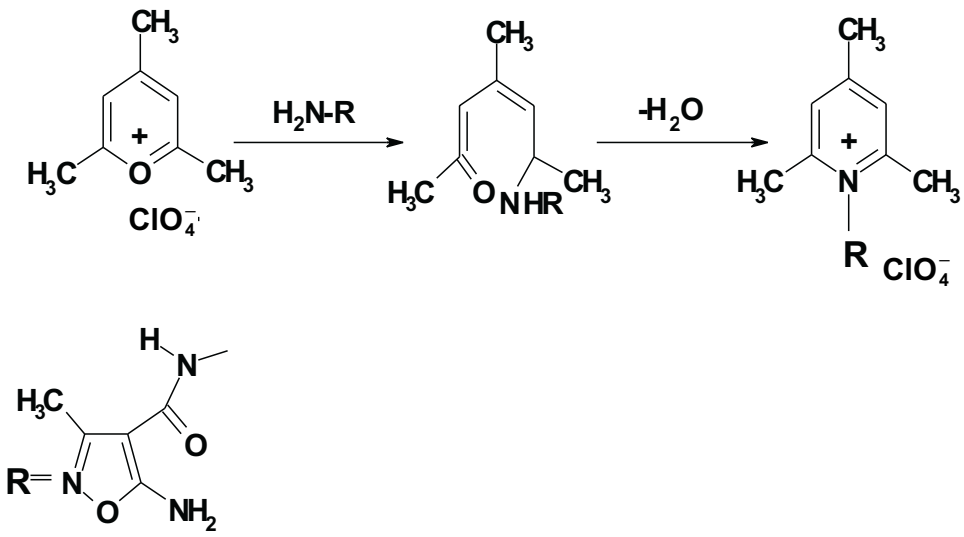

Figure 2. The scheme of synthesis of 5-amino-3-methylisoxazole-4-carboxylic acid N-(2,4,6-trimethylpyridinium)amide chlorate(VII) salt.

The melting point of **1** was 225°C (the yield was 46%). The spectroscopic results were as follows: IR (nujol) specord M–80, cm^{-1}: 1657 C=O, 1554 C=N and ^1H NMR (DMSO-d_6) Tesla 80 MHz, ppm: 2.25–2.40 (3s, 9H, $3CH_3$); 2.50 (s, 3H, CH_3 4-pyridinium); 4.28 (s, 2H, NH_2); 7.4 (m, 2H, aromatic); 9.47 (s, 1H, NH); MS: m/e 360.

X-ray diffraction measurements: X-ray diffraction studies were performed at room temperature using a CuKα radiation source (λ =1.5418 Å) and computer-controlled diffractometer KUMA KM4. A 0.15×0.15 ×0.25 mm crystal was measured. The structure was determined using 2246 reflections with $I > 2\sigma$. The structure was solved and refined using SHELXS-97 and SHELXL-97 programs [20].

CCDC No 214306 contains the supplementary crystallographic data for this paper. These data can be obtained free of charge *via* www.ccdc.cam.ac.uk/conts/retreving.html (or from the Cambridge Crystallographic Data Centre, 12, Union Road, Cambridge CB2 1EZ, UK; fax: +441223336033; or deposit@ccdc.cam.ac.uk).

Computational methodology: Quantum-chemical calculations were carried out for all the compounds presented in Figure 1. Gas-phase full geometry optimization was performed with the Gaussian 98 suite of programs [21] within the Density Functional Theory (DFT) [11,12]. The three-parameter hybrid

functional (B3LYP) with 6-31G(d,p) double-zeta valence basis set with polarization functions on hydrogen and heavy atoms was used [22]. Harmonic vibrational frequencies were calculated in order to confirm that the obtained geometry corresponded to the minimum on the potential energy surface (PES). Single-point calculations with a solvent reaction field were performed using the Polarizable Continuum Model (SCRF/PCM) proposed by Miertus and Tomasi [13,14]. Water (ε =78.39) was used as the solvent in order to describe the environmental influence on molecular properties. The electron densities and electrostatic potentials around the molecules were computed in both reaction fields [23,24,25]. Atomic charges were calculated according to Bader's theory [15] in order to characterize the quantum similarity of the molecules. The original Bader's package of programs was used [26]. In order to determine bond indices, the Wiberg analysis was performed [16,27]. In the next step, a solid state-geometry optimization was performed for the title compound because the original crystallographic data were available. Goedecker's pseudopotentials and the PBE functional [28] were used for this purpose. A cutoff energy of 40 Ry was used for the plane-wave basis-set crystal cell. The calculations were carried out using the CPMD computer program [17,18]. The geometrical parameters obtained experimentally were compared with the calculated ones and are presented in Table 1.

Table 1. Comparison of selected experimental and calculated geometrical parameters of 5-amino-3-methylisoxazole-4-carboxylic acid N-(2,4,6-trimethylpyridinium)amide chlorate(VII) salt.

Parameter	Experimental X-ray	Calculated	
		Gas-phase	Solid-state
Bond length (Å)			
C(1)–C(2)	1.482(4)	1.4987	1.5263
C(2)–C(3)	1.427(4)	1.4411	1.4651
C(3)–C(4)	1.377(3)	1.4034	1.4209
C(4)–O(5)	1.337(3)	1.3283	1.4752
O(5)–N(6)	1.439(4)	1.4385	1.5642
N(6)–C(2)	1.290(3)	1.305	1.3308
C(4)–N(7)	1.310(4)	1.3307	1.3624
C(3)–C(10)	1.446(3)	1.4325	1.4688
C(10)–O(11)	1.225(3)	1.2321	1.2629
C(10)–N(12)	1.374(3)	1.4259	1.4543
N(12)–N(14)	1.396(2)	1.3973	1.4681
Bond angle (°)			
C(1)–C(2)–C(3)	129.78	129.75	129.47
N(6)–C(2)–C(3)	112.33	112.14	113.80
C(2)–C(3)–C(4)	104.10	103.00	104.79
C(3)–C(4)–O(5)	109.37	110.06	110.87
C(4)–O(5)–N(6)	108.82	109.06	105.69
N(7)–C(4)–C(3)	132.27	130.46	131.05
N(12)–N(14)–C(15)	117.04	119.67	115.87
Torsion angle (°)			
C(1)–C(2)–C(3)–C(4)	–177.18	–179.65	–174.86
N(7)–C(4)–C(3)–C(2)	–179.00	–179.86	–177.99
C(10)–N(12)–N(14)–C(15)	94.96	87.04	89.36

RESULTS AND DISCUSSION

X-ray crystallography: The crystal is monoclinic with the space group $P2_1/c$. The unit cell dimensions are: a = 15.892 (3) Å, b = 12.230(2) Å, c = 8.548(2) Å, β = 100.92(3) deg. The final values of the R indices were R_1 = 0.0585 and wR_2 = 0.1658. There are four identical, related by symmetry 5-amino-3-methylisoxazole-4-carboxylic acid N-(2,4,6-trimethylpyridinium)amide cations as well as four chlorate(VII) anions in the crystal unit cell. The molecular structure of the 5-amino-3-methylisoxazole-4-carboxylic acid N-(2,4,6-trimethylpyridinium)amide chlorate(VII) salt is presented in Figure 3. The empirical formula of the complex is $C_{13}H_{17}ClN_4O_6$. Molecular weight and cell volume are 360.76 and 1631.3(6) Å^3, respectively. The isoxazole ring is planar within the limits of experimental error. The methyl and amine groups are co-planar with the isoxazole ring and the torsion angles C(1)–C(2)–C(3)–C(4) and N(7)–C(4)–C(3)–C(2) are –177.18° and –179°, respectively. The pyridine plane is forming an angle of 64.4° with the isoxazole ring. The peptide bond is not co-planar with the isoxazole and pyridine rings. The torsion angle C(10)–N(12)–N(14)–C(15)

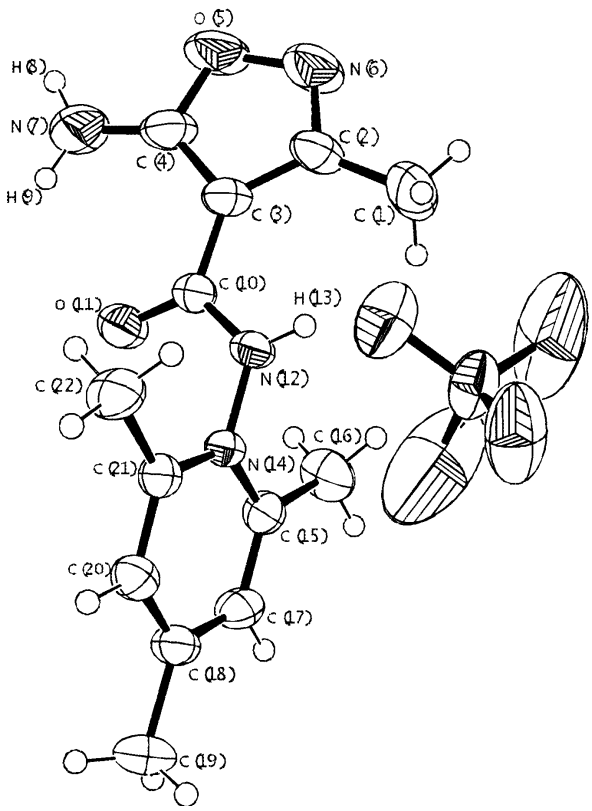

Figure 3. Crystallographic structure of 5-amino-3-methylisoxazole-4-carboxylic acid N-(2,4,6-trimethylpyridinium)amide chlorate(VII) salt.

is 95.0°. An intermolecular hydrogen bond exists between the N(12)–H(13) group and an oxygen atom of the ClO_4^- anion. The selected experimental geometrical parameters are presented in Table 1. The complete set of crystallographic data is available on request.

Molecular Modeling: The gas-phase and solvent reaction field calculations were performed for isolated molecules **1–4** (see Figure 1). The title compound **1** has an ionic form in the solid state. The ClO_4^- ions were not taken into account during the gas-phase and solvent study because the solvation process leads to dissociation into ionic forms, so only the cationic form of isoxazole derivative **1** seems to exist in majority of biological systems. The structural parameters calculated in the gas-phase for molecule **1** agree quite well with X-ray crystallography data (see Table 1). The solid-state full geometry optimization reproduces in general well the overall structure of analyzed crystal. The isoxazole ring edge, especially bonds around O(5) atom are very difficult to be correctly estimated for Goedecker's pseudopotentials used in the solid-state geometry optimization. The mean difference between experimental and calculated bond lengths is 0.05 Å. The valence and dihedral angles were reproduced very well by both approaches. The main goal in our molecular modeling study was the explanation why compound **1** does not exhibit pronounced immunological activity. It had been reported that similar compounds substituted by a phenyl ring exhibit immunological properties [4], so it seemed interesting why the compound substituted by a pyridine ring is immunologically inactive. In order to find the answer, advanced (for the molecules of this size) quantum-chemical calculations were performed using the B3LYP functional with 6-31G(d,p) double-zeta valence basis set. The experimentally obtained compounds (**1** and **2**) and the two model structures (**3** and **4**) were analyzed in our theoretical study. The differential maps of electron density and electrostatic potential, obtained by subtracting the gas-phase from the SCRF/PCM results, reflect the most sensitive places in acceptor-drug interactions and give insight into the electronic structures of the discussed molecules. The differential maps of electron density are presented in Figure 4. Dark grey regions represent an increase in electron density, and light grey a decrease in electron density upon SCRF/PCM and water ($\varepsilon = 78.39$) as a solvent treatment. The most significant differences are visible for O(5) and N(6) in the isoxazole ring edge, methyl and amino groups in all the compounds. The solvent influence on electron density is different in molecules **1** and **4** from that in **2** and **3**. Compounds **1** and **4** exhibit a redistribution of electron density along the whole peptide bond, while in compounds **2** and **3** the changes are mostly located on O(11) from the carbonyl group and on the N(12)–H(13) group. An interesting fact is that the electron density is different along the N(12)–C(14) in **2**, **3** from that along the N(12)–N(14) bonds in **1**, **4**. This is probably the result of the cationic form of compounds **1** and **4** and may have an influence on biological properties. The differential maps of electrostatic potential are presented in Figure 5. The maps were generated according to the same rules as described above. Dark grey regions represent an increase of negative, and light grey of positive electrostatic potential upon SCRF/PCM treatment. The increase of positive electrostatic potential around the O(5) and N(6) atoms

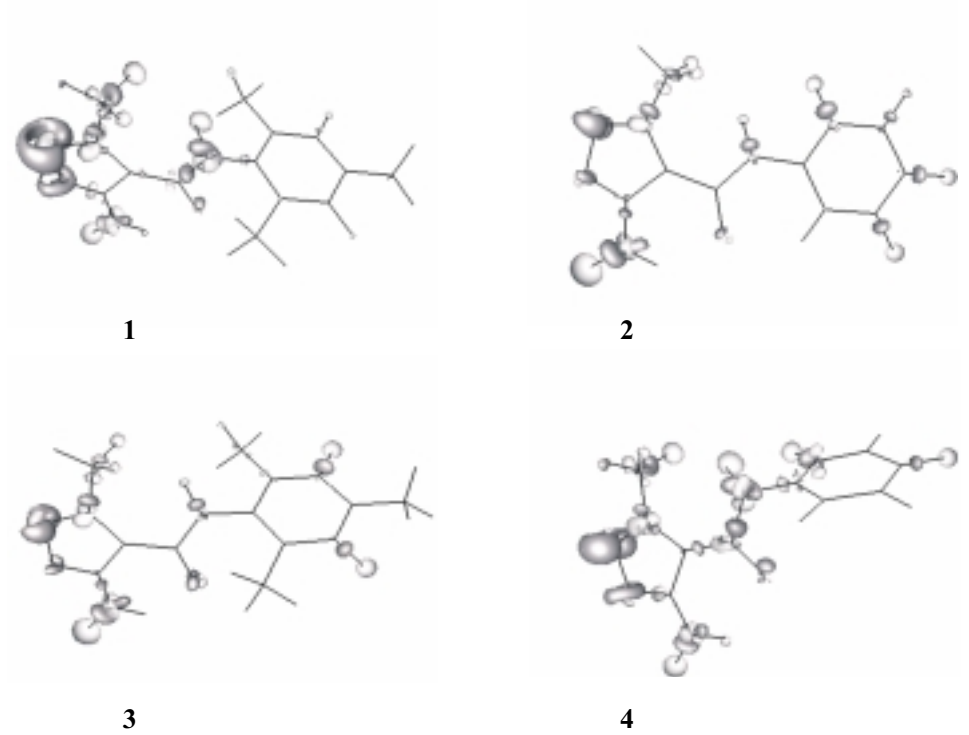

Figure 4. The differential maps of electron density around the investigated molecules generated using the DFT method with the 6-31G(d,p) basis set. Dark grey (0.002 a.u.) regions represent an increase in the electron density and light grey (–0.002 a.u.) a decrease in the electron density upon SCRF/PCM and water (ε = 78.39) as a solvent treatment.

is evident. This can suggest that the isoxazole ring edge is involved in acceptor-ligand bonding. For compounds substituted by a pyridine ring the centers of increased negative electrostatic potential are additionally visible. This can be one more possible reason why compound **1** is inactive immunologically. The compound is probably able to interact with a different acceptor. In the next step, the atomic charges were calculated according to Bader's theory. The charges calculated using the AIM scheme are not significantly dependent on the size of the basis set and the level of theory used for calculations [29]. Table 2 contains results obtained in the gas-phase and solvent reaction fields for selected atoms. The most significant differences resulting from the environment interactions are visible for the O(5), N(6), H(8) and O(11) atoms. It is thus shown that the electron density distribution changes induced by the solvent occur mostly on atoms having lone electron pairs but not shielded by other atoms, or atoms engaged in hydrogen bonds. Contrary to our expectations, no significant differences are visible for atom N(14) from the pyridine or C(14) from the phenyl rings. These atoms are shielded by a methyl group or other atoms from aromatic rings. The sums of the Wiberg bond indices for selected atoms are presented in Table 3. The most interesting is that the sum of bond orders at the N(14) atom is not exactly three, as for organic

compounds containing nitrogen atoms, nor four, as expected for a quarternary nitrogen atom. In the analyzed compounds **1** and **4** the sum of the Wiberg bond indexes is ~3.60. We can speculate that this quite strange sum of bond orders for the N(14) atom is a further reason why compound **1** does not exhibit immunological properties. It is much smaller than value of 3.96 for carbon analogues (compounds **2** and **3**). Finally we can conclude that the methods applied in this study are able to describe the electronic structure variations between experimentally obtained isoxazole derivatives with different aromatic substituents. The electron density shifts caused by the quaternary nitrogen atom can be a reason why the compound **1** does not exhibit the defined immunological activity. The solid-state geometry optimization was used as a tool to reproduce crystallographic data. The solid-state calculations are still in development, but they are very promising for detailed structural research.

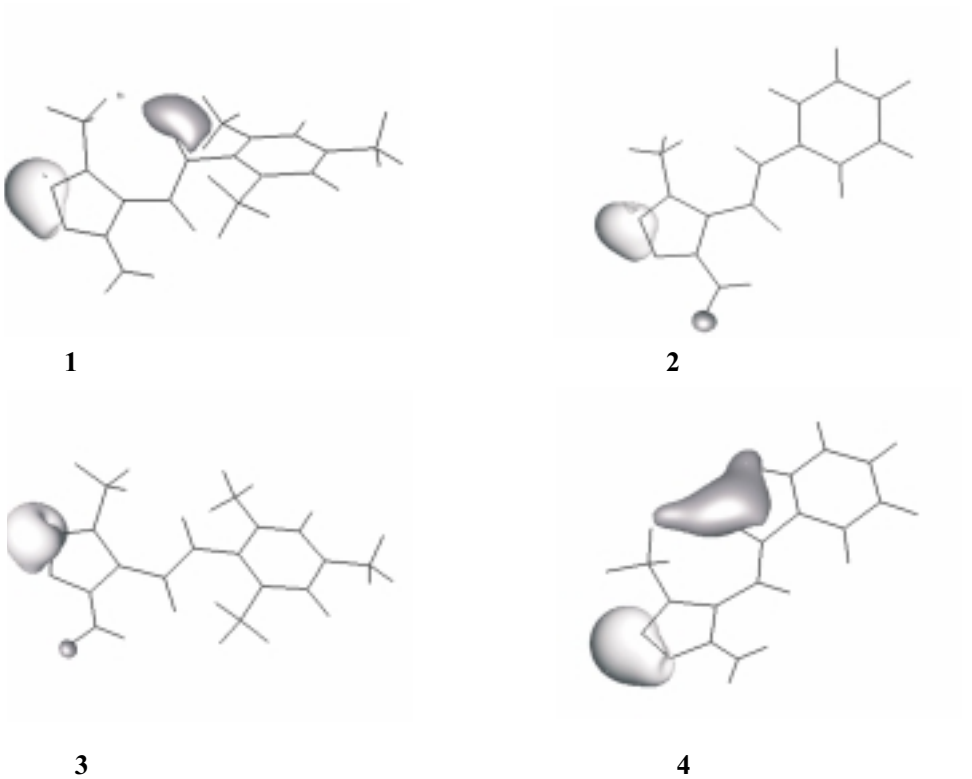

Figure 5. The differential maps of electrostatic potential around the investigated molecules generated using the DFT method with the 6-31G(d,p) basis set. Dark grey (0.02 a.u.) regions represent an increase of negative and light grey (range from –0.03 to –0.02 a.u.) of positive electrostatic potential upon SCRF/PCM and water (ε = 78.39) as a solvent treatment.

Table 2. Comparison of AIM atomic charges for selected atoms calculated in gas-phase and solvent (SCRF/PCM) reaction fields for **1–4** molecules.

Atom	Compounds							
	Gas-phase				Solvent (water ε = 78.39)			
	1	**2**	**3**	**4**	**1**	**2**	**3**	**4**
C(1)	0.077	0.077	0.078	0.075	0.068	0.066	0.070	0.065
C(2)	0.643	0.621	0.621	0.649	0.646	0.624	0.623	0.653
C(3)	–0.024	–0.026	–0.025	–0.012	–0.018	–0.031	–0.026	–0.007
C(4)	1.214	1.145	1.136	1.226	1.200	1.137	1.127	1.209
O(5)	–0.793	–0.805	–0.806	–0.791	–0.820	–0.820	–0.821	–0.819
N(6)	–0.583	–0.607	–0.610	–0.579	–0.661	–0.666	–0.669	–0.661
N(7)	–1.269	–1.261	–1.255	–1.268	–1.282	–1.270	–1.261	–1.283
H(8)	0.475	0.444	0.440	0.479	0.509	0.498	0.491	0.517
H(9)	0.505	0.509	0.508	0.505	0.517	0.512	0.510	0.509
C(10)	1.350	1.459	1.451	1.327	1.361	1.456	1.448	1.342
O(11)	–1.208	–1.213	–1.220	–1.201	–1.222	–1.232	–1.243	–1.216
N(12)	–0.755	–1.239	–1.219	–0.714	–0.751	–1.241	–1.217	–0.716
H(13)	0.444	0.403	0.400	0.449	0.470	0.421	0.418	0.480
N(14) or C(14)	–0.910	0.383	0.354	–0.941	–0.914	0.370	0.336	–0.944
C(15)	0.455	–0.005	0.028	0.500	0.457	–0.013	–0.004	0.485
C(16)	0.083	–	0.078	–	0.074	–	0.067	–
C(17)	0.041	0.014	–0.011	0.071	0.040	0.002	–0.027	0.063
C(18)	0.040	0.004	0.011	0.055	0.040	–0.012	–0.003	0.045
C(19)	0.075	–	0.080	–	0.071	–	–0.073	–
C(20)	0.042	0.009	–0.010	0.070	0.038	–0.009	–0.030	0.060
C(21)	0.482	0.015	0.007	0.540	0.481	–0.005	0.009	0.526
C(22)	0.092	–	0.075	–	0.086	–	0.074	–
C(20)	0.042	0.009	–0.010	0.070	0.038	–0.009	–0.030	0.060
C(21)	0.482	0.015	0.007	0.540	0.481	–0.005	0.009	0.526
C(22)	0.092	–	0.075	–	0.086	–	0.074	–

Table 3. Sum of Wiberg bond indices for selected atoms of the compounds **1–4**.

Atoms and numbers	Investigated compounds			
	1	**2**	**3**	**4**
C(1)	3.8069	3.8135	3.8157	3.8040
C(2)	3.9944	3.9956	3.9955	3.9940
C(3)	3.9223	3.9347	3.9349	3.9235
C(4)	3.8822	3.9956	3.8842	3.8813
O(5)	2.3265	2.3069	2.3064	2.3291

Table 3 (continuation)

N(6)	2.9212	2.9001	2.8974	2.9244
N(7)	3.0591	3.0175	3.0111	3.0676
H(8)	0.8000	0.8178	0.8193	0.7979
H(9)	0.7901	0.7918	0.7930	0.7894
C(10)	3.9002	3.8915	3.8937	3.8967
O(11)	1.9792	1.9457	1.9469	2.0014
N(12)	3.0533	3.2471	3.1933	3.0570
H(13)	0.8096	0.8261	0.8251	0.8092
N(14) or C(14)	N(14) 3.6044	C(14) 3.9598	C(14) 3.9545	N(14) 3.6446
C(15)	3.9423	3.9464	3.9984	3.8677
C(16)	3.7948	–	3.8311	–
C(17)	3.9262	3.9462	3.9439	3.9218
C(18)	3.9754	3.9453	3.9993	3.9092
C(19)	3.8023	–	3.8341	–
C(20)	3.9253	3.9465	3.9439	3.9211
C(21)	3.9325	3.9240	3.9982	3.8492
C(22)	3.7911	–	3.8245	–

The numbering scheme is the same as in the crystallographic structure.

Acknowledgments

Authors would like to thank Dr. Jarosław Panek for fruitful discussion. The project was financially supported by the Polish State Committee for Scientific Research (Grant KBN 3PO5F 01224). The Wrocław Centre for Networking and Supercomputing (WCSS) and Academic Computer Center CYFRONET-KRAKÓW (Grant KBN/SGI/UWrocl/078/2001) are gratefully acknowledged for providing computer time and facilities.

REFERENCES

1. Ryng S., Machoń Z., Wieczorek Z., Zimecki M. and Głowiak T., *Arch. Pharm. Pharm. Med. Chem.*, **330**, 319 (1997).
2. Ryng S., Malinka W. and Duś D., *Il Farmaco*, **52**, 105 (1997).
3. Ryng S. and Głowiak T., *J. Chem. Crystallogr.*, **5**, 373 (1998).
4. Ryng S., Zimecki M., Sonnenberg Z. and Mokrosz M.J., *Arch. Pharm. Pharm. Med. Chem.*, **332**, 158 (1999).
5. Ryng S., Machoń Z., Wieczorek Z. and Zimecki M., *Pharmazie*, **54**, 359 (1999).
6. Ryng S., Machoń Z., Wieczorek Z., Zimecki M. and Mokrosz M., *Eur. J. Med. Chem.*, **33**, 831 (1998).
7. Lee Y. and Kim B.H., *Bioorg. Med. Chem. Lett.*, **12**, 1395 (2002).
8. Kang Y.K., Shin K.J., Yoo H.K., Seo K.J., Hong C.Y., Lee C., Park S.Y., Kim D.J. and Park S.W., *Bioorg. Med. Chem. Lett.*, **10**, 95 (2000).
9. Eddington N.D., Cox D.S., Roberts R.R., Butcher R.J., Edafiogho I.O., Stables J.P., Cooke N., Goodwin A.M., Smith C.A. and Scott K.R., *Eur. J. Med. Chem.*, **37**, 635 (2002).
10. Szafran M., *Wiad. Chem.*, **47**, 477 (1993).
11. Hohenberg P. and Kohn W., *Phys. Rev.*, **136**, B864 (1964).
12. Kohn W. and Sham L.J., *Phys. Rev.*, **140**, A1133 (1965).
13. Miertus S. and Tomasi J., *Chem. Phys.*, **65**, 239 (1982).
14. Fortunelli A. and Tomasi J., *Chem. Phys. Lett.*, **231**, 34 (1994).

15. Bader R.F.W., "Atoms in Molecules – A Quantum Theory", Oxford University Press, Oxford, 1990.
16. Wiberg K.B., *Tetrahedron*, **24**, 1083 (1968).
17. Hartwigsen C., Goedecker J. and Hutter J., *Phys. Rev. B*, **58**, 3641 (1998).
18. *CPMD*, Hutter J. *et al*., Copyright IBM Zurich Research Laboratory and MPI für Festkörperforschung, (1995–2001).
19. Ryng S. and Głowiak T., *Synth. Commun.*, **27**, 1359 (1997).
20. Sheldrick G., SHELXS-97 and SHELXL-97: Programs for the Solution and Refinement of Crystal Structures, University of Göttingen, Germany, (1997).
21. Gaussian 98, Rev. A11, M.J. Frisch, G.W. Trucks, H.B. Schlegel, G.E. Scuseria, M.A. Robb, J.R. Cheeseman, V.G. Zakrzewski, J.A. Montgomery, R.E. Stratman, J.C. Burant, S. Dapprich, J.M. Millam, A.D. Daniels, K.N. Kudin, M.C. Strain, O. Farkas, J. Tomasi, V. Barone, M. Cossi, R. Cammi, B. Mennucci, C. Pomelli, C. Adamo, S. Clifford, J. Ochterski, G.A. Petersson, P.Y. Ayala, Q. Cui, K. Morokuma, P. Salvador, J.J. Dannenberg, D.K. Malick, A.D. Rabuck, K. Raghavachari, J.B. Foresman, J. Cioslowski, J.V. Ortiz, A.G. Baboul, B.B. Stefanov, G. Liu, A. Liashenko, P. Piskorz, I. Komaromi, R. Gomperts, R.L. Martin, D.J. Fox, T. Keith, M.A. Al-Laham, C.Y. Peng, A. Nanayakkara, M. Challacombe, P.M.W. Gill, B. Johnson, W.Chen, M.W. Wong, J.L. Andres, C. Gonzales, M. Head-Gordon, E.S. Replogle and J.A. Pople, Gaussian Inc., Pittsburgh PA, 2001.
22. Krishnan R., Binkley J.S., Seeger R. and Pople J.A., *J. Chem. Phys.*, **72**, 650 (1980).
23. HadŸi D., Koller J., Hodošček M. and Kocjan D., in: "QSAR in Drug Design and Toxicology", Elsevier, 1987.
24. Ivanciuc O., in: QSPR/QSAR Studies by Molecular Descriptors", ed. Diudea M.V., NoVa Science Inc., NY, 2000.
25. Wade R.C., in: „3D QSAR in Drug Design", ed. Kubinyi H., ESCOM, Leiden, 1993.
26. Biegler-König F.W., Bader R.F.W. and Tang T.H., *J. Comp. Chem.*, **3**, 317 (1982).
27. Glendening E.D., Reed A.D., Carpenter J.E. and Weinhold F., NBO Version 3.1.
28. Perdew J.P., Burke K. and Ernzerhof M., *Phys. Rev. Lett.*, **77**, 3865 (1996).
29. Popelier P.L.A., "Atoms in Molecules. An Introduction", Pearson Education, Harlow, 2000.